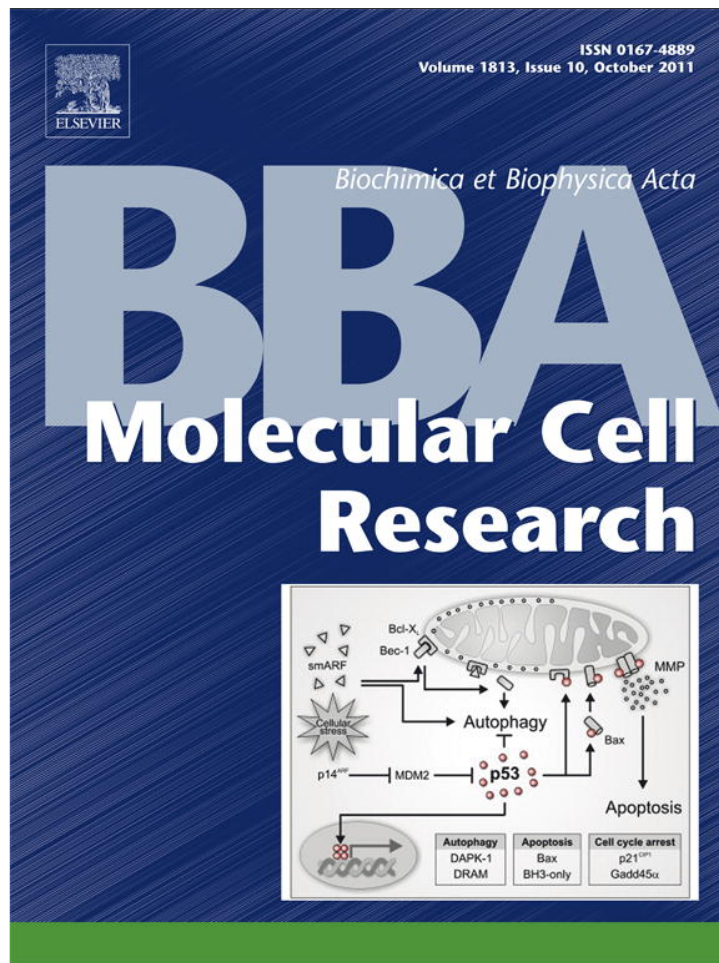


Provided for non-commercial research and education use.  
Not for reproduction, distribution or commercial use.



This article appeared in a journal published by Elsevier. The attached copy is furnished to the author for internal non-commercial research and education use, including for instruction at the authors institution and sharing with colleagues.

Other uses, including reproduction and distribution, or selling or licensing copies, or posting to personal, institutional or third party websites are prohibited.

In most cases authors are permitted to post their version of the article (e.g. in Word or Tex form) to their personal website or institutional repository. Authors requiring further information regarding Elsevier's archiving and manuscript policies are encouraged to visit:

<http://www.elsevier.com/copyright>



Contents lists available at ScienceDirect

Biochimica et Biophysica Acta

journal homepage: [www.elsevier.com/locate/bbamcr](http://www.elsevier.com/locate/bbamcr)

## Direct interaction of the Usher syndrome 1G protein SANS and myomegalin in the retina

Nora Overlack<sup>a</sup>, Dilek Kilic<sup>a,1</sup>, Katharina Bauß<sup>a</sup>, Tina Märker<sup>a,2</sup>, Hannie Kremer<sup>b,c,d</sup>, Erwin van Wijk<sup>b,c,d</sup>, Uwe Wolfrum<sup>a,\*</sup>

<sup>a</sup> Institute of Zoology, Cell and Matrix Biology, Johannes Gutenberg University of Mainz, 55099 Mainz, Germany

<sup>b</sup> Department of Otorhinolaryngology, The Netherlands

<sup>c</sup> Nijmegen Centre for Molecular Life Sciences, The Netherlands

<sup>d</sup> Donders Institute for Brain, Cognition and Behaviour, Radboud University Nijmegen Medical Centre, 6500 HB Nijmegen, The Netherlands

### ARTICLE INFO

#### Article history:

Received 13 April 2011

Received in revised form 18 May 2011

Accepted 19 May 2011

Available online 13 July 2011

#### Keywords:

Sensorineuronal degeneration

Photoreceptor cell function

Intracellular transport

Microtubule based transport

Phosphodiesterase 4D interacting protein (PDE4DIP)

### ABSTRACT

The human Usher syndrome (USH) is the most frequent cause of combined hereditary deaf-blindness. USH is genetically heterogeneous with at least 11 chromosomal loci assigned to 3 clinical types, USH1-3. We have previously demonstrated that all USH1 and 2 proteins in the eye and the inner ear are organized into protein networks by scaffold proteins. This has contributed essentially to our current understanding of the function of USH proteins and explains why defects in proteins of different families cause very similar phenotypes. We have previously shown that the USH1G protein SANS (scaffold protein containing ankyrin repeats and SAM domain) contributes to the periciliary protein network in retinal photoreceptor cells. This study aimed to further elucidate the role of SANS by identifying novel interaction partners. In yeast two-hybrid screens of retinal cDNA libraries we identified 30 novel putative interacting proteins binding to the central domain of SANS (CENT). We confirmed the direct binding of the phosphodiesterase 4D interacting protein (PDE4DIP), a Golgi associated protein synonymously named myomegalin, to the CENT domain of SANS by independent assays. Correlative immunohistochemical and electron microscopic analyses showed a co-localization of SANS and myomegalin in mammalian photoreceptor cells in close association with microtubules. Based on the present results we propose a role of the SANS-myomegalin complex in microtubule-dependent inner segment cargo transport towards the ciliary base of photoreceptor cells.

© 2011 Elsevier B.V. All rights reserved.

### 1. Introduction

The human Usher syndrome (USH) is the most frequent cause of combined hereditary deaf-blindness. USH is genetically heterogeneous with at least 11 chromosomal loci involved [1,2]. Depending on the degree of clinical symptoms, USH can be divided into 3 types USH1, USH2, and USH3 [3–5]. USH1 represents the most severe form, characterized by profound congenital deafness, vestibular dysfunction and prepubertal-onset of *retinitis pigmentosa* (RP) [1,6].

The gene products of the 9 so far identified USH genes are assigned to various protein classes and families [1,6,7]. The *USH1B* gene encodes the molecular motor myosin VIIa. Harmonin (*USH1C*), SANS (scaffold

protein containing ankyrin repeats and SAM domain, *USH1G*) and whirlin (*DFNB31/USH2D*) belong to the group of scaffold proteins [2,8] and reviewed in [1,6]. Cadherin 23 (*CDH23/USH1D*) and protocadherin15 (*PCDH15/USH1F*) are cell–cell adhesion proteins, whereas *USH2A* and *GPR98* encode large transmembrane proteins, the *USH2A* isoform b and the very large G protein coupled receptor 1b/G protein-coupled receptor 98 (VLGR1b/*GPR98*). The four-transmembrane-domain protein clarin-1 (*USH3A*) encoded by *CLRN1* is so far the only identified member of USH3 (reviewed in [1,6,7]).

Previous analyses elucidated the assembly of all USH1 and USH2 proteins into USH protein networks mediated by the USH scaffold proteins harmonin, whirlin and SANS (reviewed in [1,6,7]). In inner ear hair cells the USH protein network is essential for the correct development of hair bundle stereocilia and for signal transduction [7,9–12]. Since, in the retina, all proteins of the USH network are found at the synapse of photoreceptor cells, a role of this network in maintaining the synaptic integrity was proposed [1,6,7]. More recently, we and others have demonstrated a USH protein network organized by whirlin and SANS in the ciliary–periciliary region of photoreceptor cells [13–17]. This region connects the biosynthetic

\* Corresponding author at: Johannes Gutenberg University, Institute of Zoology, Cell and Matrix Biology, Müllerweg 6, D-55099 Mainz, Germany. Tel.: +49 6131 39 25148; fax: +49 6131 39 23815.

E-mail address: [wolfrum@uni-mainz.de](mailto:wolfrum@uni-mainz.de) (U. Wolfrum).

<sup>1</sup> Current address: Sabanci University Faculty of Engineering and Natural Sciences Biological Sciences & Bioengineering Program, 34956 Istanbul, Turkey.

<sup>2</sup> Current address: Institute for Clinical Diabetology, German Diabetes Center, Leibniz Center for Diabetes Research at the Heinrich-Heine-University Düsseldorf, Germany.

active inner segment with the photosensitive outer segment and is crucial for transport processes between these two compartments of photoreceptor cells [18]. Our previous results indicated that the USH1G protein SANS serves as a molecular interconnector between the microtubule based transport across the inner segment to the ciliary transport in the USH protein network of photoreceptor cells [13]. We have previously shown interactions of SANS with e.g. whirlin, myosin VIIa and its homomerization [13,19]. In COS7 cells SANS is recruited to the plasma membrane by USH1 cadherins, cadherin 23 and proto-cadherin 15, indicating a physical linkage of these molecules [20]. These interactions underline the SANS scaffolding function in the USH interactome and identified SANS as one of the key organizers of the ciliary–periciliary USH protein network of vertebrate photoreceptor cells [13,19]. Furthermore, we provided first evidence for an association of SANS with microtubules linking the USH protein networks to the microtubule cytoskeleton and hence to microtubule-associated intracellular transport processes [13,19]. More recently, the association of USH protein networks including SANS with transport vesicles has been demonstrated [21] confirming the latter hypothesis.

The *USH1G* gene product SANS is composed of defined domains (Fig. 1A) supposed to mediate protein–protein interactions [8]. Three N-terminal ankyrin repeats are followed by a central domain (CENT), a SAM (sterile alpha motif) domain and a class I PBM (PDZ-binding motif) at the C-terminus. The identity of the ankyrin repeats, the SAM and PBM domain, as well as their roles in protein–protein interactions have been previously studied [8,13,19]. Preceding work showed a direct interaction of the SAM domain with the PDZ domains of harmonin and whirlin *in vitro* [13,19]. In addition, a recent study revealed a synergistic binding of the SAM domain and the C-terminal PBM to the N-domain and PDZ1 of harmonin [22].

Although sequence analyses and database search described the CENT domain of SANS as an unknown or low complexity region ([www.smart.heidelberg.de](http://www.smart.heidelberg.de)), previous studies characterized it as a potent scaffold domain: preceding work demonstrated interaction of the SANS CENT domain with both MyTH4 (myosin tail homology 4) and FERM (4.1, ezrin, radixin, moesin) tandem domain repeats of myosin VIIa [19,23]. Moreover, the CENT domain is capable of mediating SANS homomerization [19]. In order to identify additional putative binding partners interacting with the CENT domain of SANS we performed

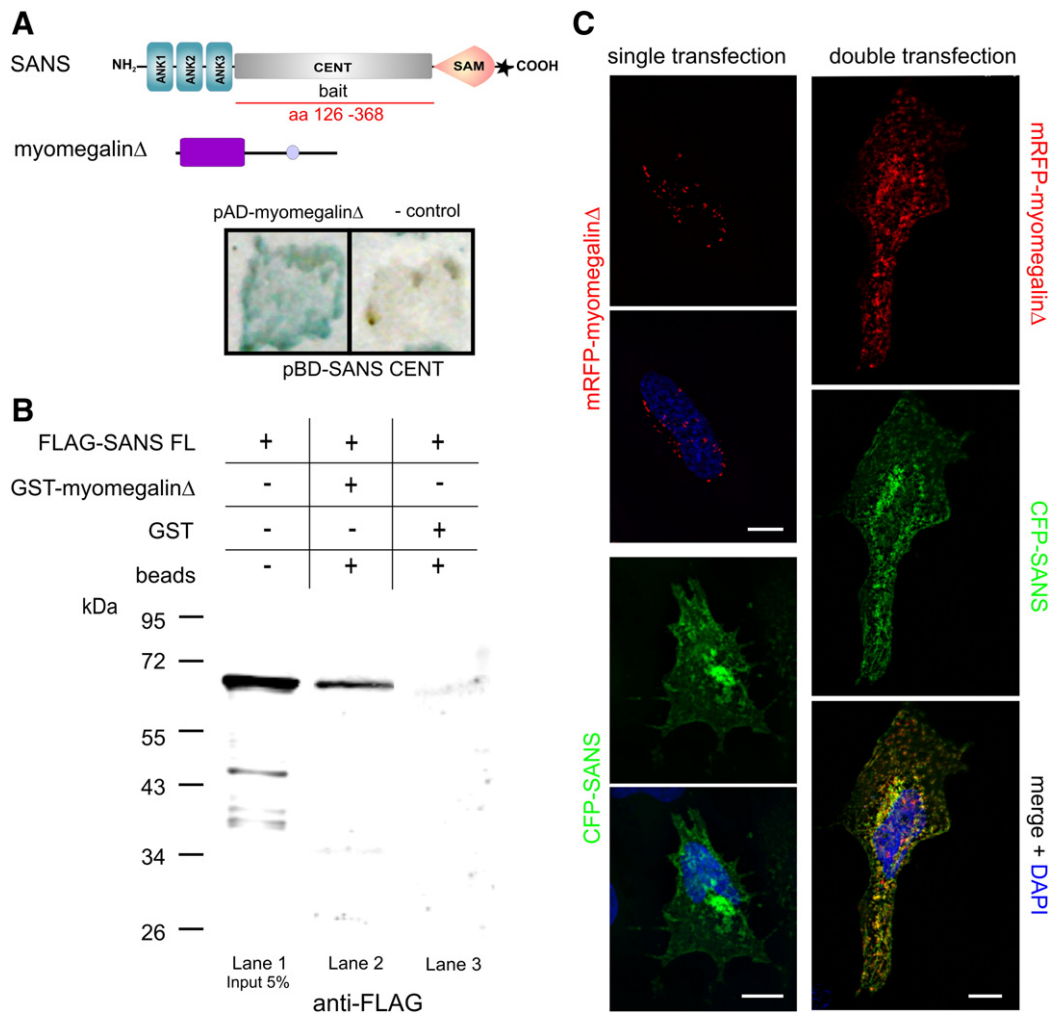


**Fig. 1.** Validation of the SANS-myomegalin interaction. (A) Scheme of SANS and myomegalinΔ domain structure and yeast two-hybrid assay. SANS is composed of three ankyrin repeats (ANK) at the N-terminus, a central domain (CENT) followed by a sterile alpha motif (SAM) and a PDZ-binding motif (PBM) at the C-terminus (asterisk). MyomegalinΔ (474 aa) contains a SCOP domain: d1gw5b (box) and coiled-coil domains (circle). Yeast two-hybrid screens were performed in a bovine retina cDNA library with SANS CENT fused to the DNA-binding domain of the GAL4 reporter. MyomegalinΔ protein was identified as one interaction candidate. (B) GST pull-down of SANS and myomegalinΔ. FLAG-tagged SANS was incubated with immobilized GST-myomegalinΔ, or GST alone. Anti-FLAG Western blot revealed pull-down of SANS by GST-myomegalinΔ (lane 2) but not GST alone (lane 3). Lane 1 shows 5% input of FLAG-SANS full length. (C) Co-localization of mRFP-myomegalinΔ and CFP-SANS in HeLa cells. Upper left panel: overexpressed mRFP-myomegalinΔ (red) is localized right around the DAPI stained nucleus in single transfected cells. Lower left panel: overexpressed CFP-SANS (green) is localized to the cytoplasm, enriched at the membrane, and as an intense spot at the periphery of the nucleus. Right panel: in mRFP-myomegalinΔ and CFP-SANS co-transfected HeLa cells, overexpressed CFP-SANS (green) recruits mRFP-myomegalinΔ (red) to the cytoplasm and an intense spot at the periphery of the nucleus. Scale bars: 10 μm.

yeast two-hybrid screens of a retinal cDNA library using the CENT domain as bait. We succeeded to identify 30 potential binding partners to SANS including myomegalin as the major SANS CENT interacting partner, most abundantly found in the screen (Fig. 1A). Myomegalin, also known as PDE4DIP (phosphodiesterase 4D interacting protein), was first identified as a novel Golgi apparatus and centrosome associated protein termed after its large size and high abundance in the muscle [24]. Data base analyses predict four isoforms for mouse myomegalin ranging in their predicted molecular weight from 15 kDa (isoform 3) to 275 kDa (isoform 1), all containing protein–protein interaction domains.

In the present study we demonstrate that myomegalin is integrated into the multifunctional protein interactome related to USH via its binding to the USH scaffold protein SANS. The SANS–myomegalin interaction was confirmed by independent assays and partial co-localization of the interacting partners was shown in mammalian retinas. Conclusively, the present data also provide further insights on the role of the SANS organized protein complex in microtubule-based inner segmental cargo transport.

## 2. Methods

### 2.1. Yeast two-hybrid screen

The yeast two-hybrid screen was performed as previously described [13]. The CENT domain of SANS (amino acids 126–368) was used as bait on a bovine oligo-dT primed retinal cDNA library. Interactions were analyzed by assessment of reporter gene activation. If yeast clones grew on selection plates and were stained in the  $\alpha$ - and  $\beta$ -galactosidase activity assays, an interaction between a protein pair was indicated.

### 2.2. GST pull-down assays

Bovine myomegalin $\Delta$  clone, found in the yeast two-hybrid, was subcloned in the pGEX4T3 vector, expressed in *E. coli* BL21 and bound to beads as described in [25]. FLAG-tagged human SANS full length (amino acids 1–461) was produced by transfection of COS-7 cells with the appropriate vector, using Lipofectamine<sup>TM</sup> LTX and Plus Reagent as transfection reagent (Invitrogen, Karlsruhe, Germany) according to manufacturer's instructions. 24 h post-transfection cells were washed with PBS and subsequently lysed on ice in lysis buffer (50 mM Tris–HCl pH 7.5, 150 mM NaCl, and 0.5% Triton-X-100). The cell supernatant was incubated 2 h at 4 °C with equal amounts of beads pre-incubated either with GST or with GST-fusion proteins. Beads were washed with lysis buffer and precipitated protein complexes were eluted with SDS sample buffer and subjected to SDS-PAGE and Western blot.

### 2.3. Antibodies

Polyclonal SANS antibodies generated against a murine fragment (amino acids 1–46) and raised in rabbit were previously characterized [14]. Anti-Myomegalin polyclonal mouse antibody (H00009659-B01) and anti-FLAG-tag antibodies were acquired from Abnova (Taiwan) or Sigma-Aldrich (Sigma-Aldrich, St. Louis, MO, USA), respectively. Monoclonal antibodies against centrin 3 were previously reported [26]. Secondary antibodies were purchased from Invitrogen or Rockland.

### 2.4. Animals and tissue preparation

All experiments described herein conform to the statement by the Association for Research in Vision and Ophthalmology (ARVO) as to care and use of animals in research. Adult C57BL/6J mice were maintained under a 12 h light–dark cycle, with food and water *ad*

*libitum*. After sacrifice of the animals in CO<sub>2</sub> (rodents) and decapitation, subsequently entire eyeballs, and appropriate tissues were dissected, or retinas were removed through a slit in the cornea prior to further analysis. Eyes of *macaca mulatta* were obtained from the German Primate Center (DPZ, Göttingen, Germany). Human eyes were obtained from the Dept. of Ophthalmology, Mainz, Germany and guidelines to the declaration of Helsinki were followed.

### 2.5. Fluorescence microscopic analysis of transfected HeLa cells

Human full-length SANS was cloned in pPalm-Myr-CFP vector resulting in an N-terminal CFP-fusion protein. Bovine myomegalin $\Delta$  was cloned in pDest-733 (Invitrogen) resulting in N-terminal fused mRFP. Both constructs were transfected individually or in combination using Lipofectamine<sup>TM</sup> LTX and Plus Reagent transfection reagent (Invitrogen) according to the manufacturer's instructions. After 24 h cells were fixed with methanol + 0.05% EGTA and air-dried. Subsequently, the samples were incubated with 0.01% Tween 20 in PBS for 20 min. After washing once with PBS, the samples were incubated in PBS with DAPI (4',6-Diamidin-2'-phenylindoldihydrochlorid) (Sigma-Aldrich) for 1 h at room temperature in the dark. After washing with PBS sections were mounted in Mowiol 4.88 (Hoechst, Frankfurt, Germany). Samples were analyzed with a Leica DM 6000 B microscope (Leica microsystems, Bensheim, Germany) and images were processed with Adobe Photoshop CS (Adobe Systems, San Jose, CA, USA).

### 2.6. Western blot analyses

For Western blot analyses, the appropriate tissue samples were prepared in RIPA buffer (50 mM Tris–HCl, 150 mM NaCl, 0.1% SDS, 2 mM EDTA, 1% NP-40, 0.5% sodium-deoxycholate, 1 mM sodiumvanadate, 30 mM sodium-pyrophosphate, pH 7.4) containing a protease inhibitor cocktail (Roche Diagnostics, Risch, Suisse). For denaturing gel electrophoresis, samples were mixed with SDS-PAGE loading buffer (10% glycerine, 250 mM Tris-base, 2% SDS, 0.5 mM EDTA, 0.001% bromophenol blue, HCl pH 8.5). For myomegalin expression analyses 75  $\mu$ g of each protein extract were separated on Mini-Protean<sup>®</sup> TGX<sup>TM</sup> 4–20% gels (Bio-Rad, Hercules, California, USA). For GST pull-down the samples were separated on a 12% polyacrylamide gel. Proteins were transferred to polyvinylidene difluoride membranes (Millipore, Schwalbach, Germany). After blocking the membrane with AppliChem blocking reagent (AppliChem, Darmstadt, Germany) for 2 h at room temperature, immunoreactivities were detected by applying primary and appropriate secondary antibodies Alexa Flour 680 (Invitrogen) or IR Dye 800 (Rockland, Gilbertsville, USA) employing the Odyssey infra red imaging system (LI-COR Biosciences, Lincoln, NE, USA).

### 2.7. RT-PCR analyses

Total RNA was isolated from mouse tissues by Macherey-Nagel RNA isolation kit (Macherey-Nagel, Düren, Germany). Reverse transcription was performed with 5  $\mu$ g of RNA with the SuperScript III First Strand kit (Invitrogen) following manufacturer's instructions with a mixture of random hexamers and oligo-dT primers. PCR was performed in a volume of 50  $\mu$ l using 2  $\mu$ l of prepared cDNA according to directions and 10 nmol of each primer/reaction. Cycling conditions were 40 cycles at 94 °C for 1 min, 50 °C for 40 s, and 72 °C for 90 s followed by a 7 min 72 °C extension. The length of PCR products was determined on 1% agarose gels. As DNA marker, a 1-kb DNA ladder (GeneCraft, Lüdinghausen, Germany) was used. Primers, specific for mouse myomegalin isoforms used for RT-PCR: Isoform 1; forward (5'-TG GAGAAGTGCTGAGAGGGTTC-3') and reverse primer (5'-CTCTGAGC-CAGTGCCTCAGAAT-3'). Isoform 2; forward (5'-AGGCAAGATGTCTCTCGT-3') and reverse primer (5'-GCATCCAGAGACTCCACCGA-3'). Isoform 3; forward (5'-ATGAGCAGACCTGGCCAG-3') and reverse primer (5'-



Sequence analyses of the 123 positive clones obtained in the Y2H assay revealed that 47 of these clones encoded for myomegalin. The identified clones contained overlapping sequences of myomegalin cDNA spanning the amino acids 577–1050 of the bovine sequence (myomegalin $\Delta$ , Fig. 1A). The interacting part of the bovine myomegalin displays 89% similarity to human and 85% similarity to mouse myomegalin. Database analysis of the myomegalin $\Delta$  interaction domain found in the Y2H screen predicted a SCOP family d1gw5b\_domain (ARM repeat superfamily) and a coiled-coil domain ([www.smart.heidelberg.de](http://www.smart.heidelberg.de)) (Fig. 1A).

### 3.2. Confirmation of direct interaction of SANS and myomegalin by GST pull-down and in cell culture

We performed GST pull-down assays and cell culture transfection assays to further validate the interaction between SANS and myomegalin *in vitro* and in cultured cells (Fig. 1B, C). Recombinant GST-myomegalin $\Delta$  fusion protein and GST alone were immobilized onto glutathione sepharose beads and incubated with FLAG-SANS full length protein. Subsequently, recovered proteins were analyzed by Western blot using anti-FLAG antibodies. GST-myomegalin $\Delta$  was able to pull-down FLAG-SANS full length (Fig. 1B), whereas GST alone was not. These data confirmed the direct interaction between SANS and myomegalin *in vitro*.

Next we analyzed whether myomegalin and SANS also interact in the cellular context. For this, we co-transfected HeLa cells with myomegalin $\Delta$  and SANS fluorescent fusion constructs. Cells expressing the mRFP-myomegalin $\Delta$  fusion proteins showed a peri-nuclear staining (Fig. 1C, upper left panel). Single transfection of HeLa cells with CFP-SANS resulted in CFP fluorescence in the cytoplasm and as a bright spot at the nucleus (Fig. 1C). Co-transfection of mRFP-myomegalin $\Delta$  and CFP-SANS induced the redistribution of mRFP-myomegalin $\Delta$  to the cytoplasm, enriched at the plasma membrane and the nuclear membrane, co-localizing with CFP-SANS (Fig. 1C). In conclusion, the *in vitro* GST pull-down and the analysis of co-transfected HeLa cells confirmed the direct binding of SANS and myomegalin.

### 3.3. Expression profile of myomegalin isoforms in different mouse tissues

PubMed database searches predicted four isoforms of myomegalin in the mouse (Fig. 2A). Isoform 1 represents the longest transcript and encodes a protein of an estimated molecular mass of 275 kDa. Isoforms 2 and 3 are much shorter, with estimated molecular weights of 126 kDa and 15 kDa, respectively. Isoform 4 also encodes for a relative large 262 kDa protein but in comparison to isoform 1 it contains a different 5' untranslated segment and lacks 5' coding sequence segments. It is of note that, isoform 4 was recently withdrawn from the PubMed database.

We analyzed the expression of myomegalin isoforms on the transcriptional level in diverse mouse tissues by RT-PCR using isoform specific primer combinations (Fig. 2B). The expression of the myomegalin isoforms varied in the different tissues tested. For example isoform 2 was detected in the retina, the olfactory epithelium, the brain, the kidney, and the lung. The long isoform 4 was expressed in the retina, the cochlea, the kidney, the heart and the muscle and thereby showed a different tissue expression profile than the similar other long isoform, isoform 1. Next we evaluated the protein expression profile of myomegalin in mouse retina and muscle. Our Western blots with antibodies against myomegalin revealed the three larger isoforms in varying amounts in the tissues analyzed. In the retina these isoforms were detected at their estimated sizes (Iso1 ~275 kDa; Iso2 ~126 kDa; Iso4 ~262 kDa) (Fig. 2C).

### 3.4. Spatial distribution of myomegalin expression in the mammalian retina

The eye is one of the main organs affected by the human Usher syndrome (USH). Previous studies indicated that the USH1G scaffold protein SANS contributes to USH protein networks and to transport processes in photoreceptor cells [13,14]. To elucidate the spatial distribution of myomegalin expression in the mammalian retina we subjected longitudinal cryosections of mouse, non-human primate (macaque), and human retinas to indirect immunofluorescence using antibodies against myomegalin (Fig. 3). Microscopic analyses

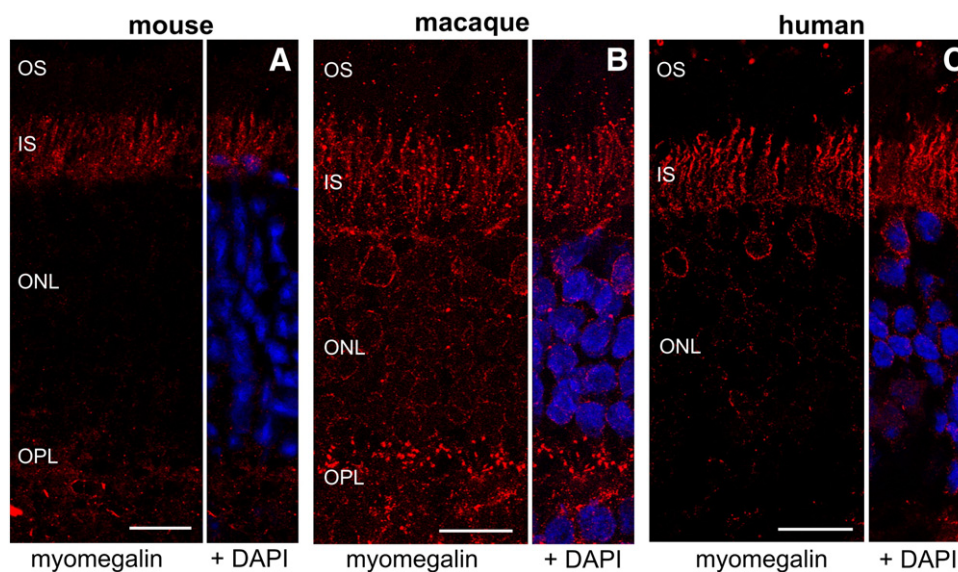


**Fig. 3.** Myomegalin expression in the retina of mouse, macaque and human. (A–C) Indirect immunofluorescence analyses of myomegalin (red) in longitudinal retina sections. Nuclear DAPI staining reveals the different layers of the retina. (A) In mouse retina myomegalin is localized in a fibrous pattern in the inner segment (IS) and is also found in the outer plexiform layer (OPL). (B) In macaque retina myomegalin is found in a fibrous pattern in the IS, where it is located around the nuclei in the outer nuclear layer (ONL) and in the OPL. (C) In human retina myomegalin is localized in a fibrous pattern in the IS, and is found around the nuclei in the outer nuclear layer (ONL). OS; outer segment. Scale bars: 15  $\mu$ m.

revealed myomegalin staining in different layers of the mammalian retina; the outer plexiform layer, the outer nuclear layer, the outer limiting membrane, and the photoreceptor layer where it was present in the inner segment and the region of the connecting cilium (Fig. 3A, B). The myomegalin staining of the perinuclear cytoplasm was more prominent in the outer nuclear layer of macaque and human retinas (Fig. 3B, C) in comparison to the mouse retina (Fig. 3A). The unconventional localization of myomegalin in the perinuclear cytoplasm was confirmed in higher resolution immunofluorescence analysis and immunoelectron microscopy of human photoreceptor cells (Fig. 4). It is notable that the synapses in the outer plexiform layer were barely stained by anti-myomegalin in the analyzed human retina specimens (Fig. 3C). This is most probably due to post-mortem proteolytic degradation of the synaptic regions in the human donor eyes frequently observed by electron microscopic analysis (data not shown).

Since in previous studies a ciliary-periciliary USH protein network was demonstrated in photoreceptor cells [13,15–17] we next focused on a putative ciliary association of myomegalin. For this we double labeled retinal sections with antibodies against myomegalin and

centrin, a validated marker for the connecting cilium, its basal body and the adjacent centriole of photoreceptor cells (Fig. 5). Myomegalin was stained in a punctuated pattern throughout the entire inner segment. Merged images revealed that the myomegalin staining overlaps with the anti-centrin immunofluorescence in the apical inner segment tips at the base of the connecting cilium, indicating the localization of myomegalin in the basal body and the adjacent centriole (Fig. 5).

### 3.5. Co-localization of myomegalin and SANS in retinal photoreceptor cells

A prerequisite for functional interactions of two proteins *in vivo* is that both are co-expressed in the same cell of a tissue and are co-localized in same subcellular compartment of this cell type. Previously published data [13,14] and present results on the spatial distribution of the interacting partners SANS and myomegalin indicated co-expression in retinal photoreceptor cells. To evaluate potential co-localization of the interacting partners we performed double immunofluorescence analyses on longitudinal sections

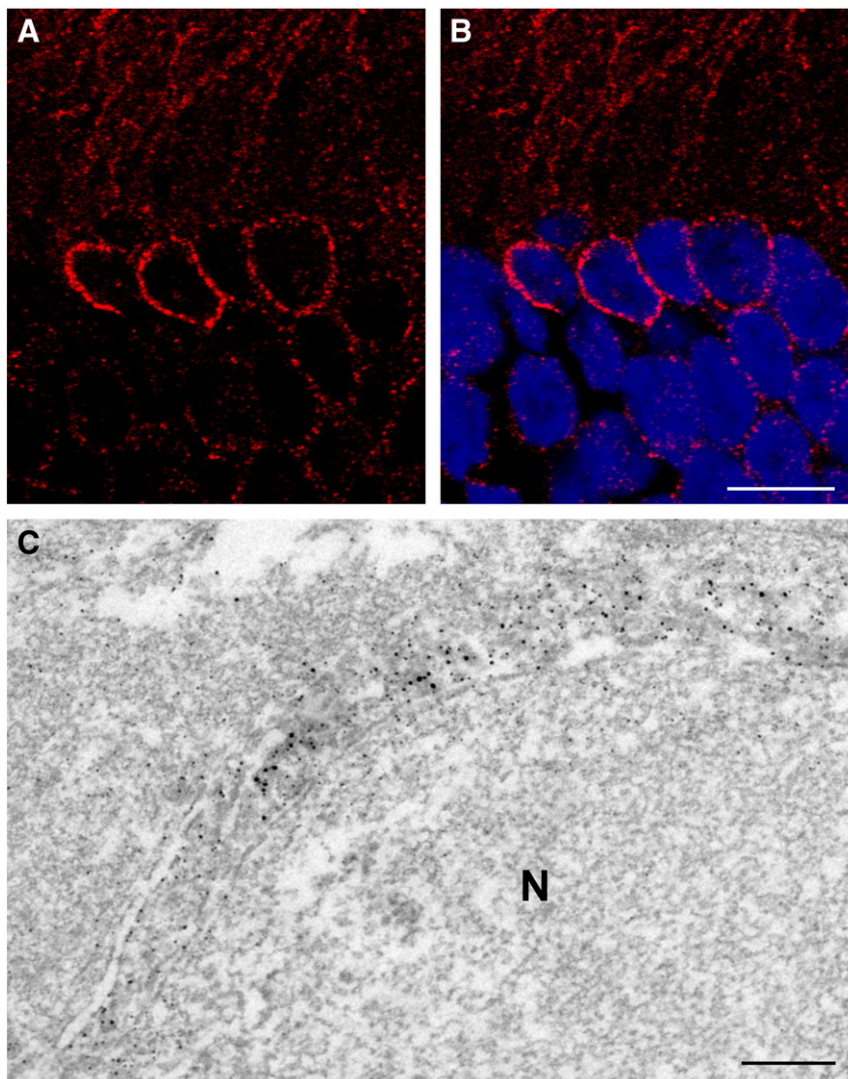


**Fig. 4.** Localization of myomegalin around the nucleus of photoreceptor cells by indirect immunofluorescence and immunoelectron microscopy. (A, B) Anti-myomegalin labeling (red) demonstrates localization of myomegalin around the nuclei (blue) of human photoreceptor cells. (C) Labeling of anti-myomegalin antibodies is detected around the nucleus of a human photoreceptor cell by immunoelectron microscopy. Scale bars: A, B: 7.5  $\mu$ m; C: 250 nm.

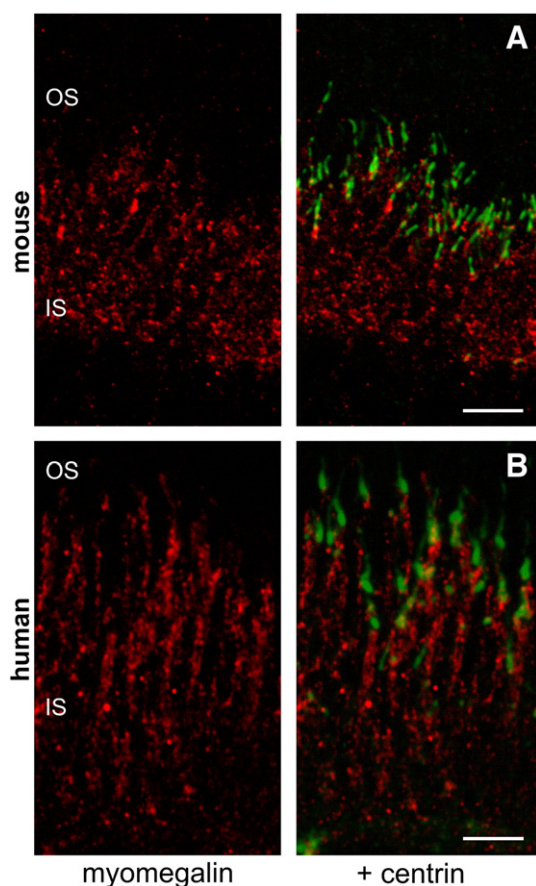


**Fig. 5.** Localization of myomegalin and centrin in mouse and human photoreceptor cells. (A) Indirect immunofluorescence of myomegalin and centrin as a marker for the connecting cilium and adjacent centriole on longitudinal sections through mouse retina. Confocal image shows myomegalin (red) localization as fibrous pattern in the inner segment. Overlay with centrin (green) shows partial co-localization of myomegalin with centrin in the region of the basal body and centriole. (B) Indirect immunofluorescence of myomegalin and centrin as a marker for the connecting cilium and adjacent centriole on longitudinal sections through human retina. Confocal image shows myomegalin (red) localization as fibrous pattern in the inner segment. Overlay with centrin (green) shows partial co-localization of myomegalin with centrin in the region of the basal body and centriole. Scale bars: 5  $\mu$ m.

through mouse, macaque, and human retinas (Fig. 6). As already shown by single labeling of myomegalin in Fig. 3, myomegalin staining was present in the inner segment and in the peri-nuclear cytoplasm of photoreceptor cells as well as in the outer limiting membrane and at the synapses in the outer plexiform layer (Fig. 6A). Double immunofluorescence analyses revealed that myomegalin and SANS were partially co-localized in the inner segment, at the outer limiting membrane and in the periciliary region of photoreceptor cells (Fig. 6A–D). In addition, we found partial co-localization of both proteins in the outer plexiform layer of mouse retina (Fig. 6A).

Although, the analysis of higher magnifications further elucidated co-localization of SANS and myomegalin in the inner segment and at the base of the connecting cilium (Fig. 6) a more precise detection was reserved to the high resolution of electron microscopy. For the precise localization of SANS and myomegalin in photoreceptor cells we performed pre-embedding immunoelectron microscopy of human retinas (Fig. 7). The parallel analyses of ultra thin sections revealed SANS and myomegalin antibody labeling in the apical inner segment extension and in the apical part of the connecting cilium (Fig. 7A, C). On the electron micrographs SANS and myomegalin were additionally

localized along longitudinally orientated tracks spanning the inner segment (Fig. 7B, D). Post-embedding immunogold labeling of human retina ultra thin sections with anti-tubulin antibodies enabled us to identify these tracks as microtubules (Fig. 7E, F). As shown in Fig. 7E and F tubulin was also decorated in the microtubule cytoskeleton of the connecting cilium and in the apical inner segment.

#### 4. Discussion

In this study, we demonstrate that myomegalin (phosphodiesterase 4D interacting protein, PDE4DIP) directly interacts with the USH1G protein SANS and that these proteins co-localize at distinct sites in mammalian photoreceptor cells. Three independent lines of evidence show that SANS and myomegalin can form a complex *in vivo*. First, among all 30 different clones identified in the yeast two-hybrid assay as putative binding partners to SANS, clones encoding for myomegalin were the most abundant. Second, GST pull-downs confirmed the direct interaction of myomegalin with SANS *in vitro*. Third, co-transfection of mRPF-myomegalin and CFP-SANS resulted in redistribution of mRPF-myomegalin and its co-localization with CFP-SANS. In addition, *in situ* expression analyses by indirect immunofluorescence and immunoelectron microscopy localization studies of SANS and myomegalin demonstrate the co-localization of both proteins in retinal photoreceptor cells providing evidence for the assembly of SANS-myomegalin interactions/complexes *in vivo*.

The direct binding of myomegalin to SANS is most probably mediated by the interaction of the SANS CENT domain with the myomegalin ARM domain composed of Armadillo repeats (Fig. 1A). In other proteins ARM domains are potent target sites mediating the binding to diverse interacting partners [29]. Sequence analysis of the myomegalin clone gained in our present yeast two-hybrid screen predicts a SCOP family d1gw5b ARM domain as well as a coiled-coil domain (see Fig. 1A). Latter coiled-coil motifs in proteins commonly interact with coiled-coil domains of the binding partner [30,31]. However, SANS does not possess any coiled-coil domain and the interaction of the SANS CENT domain with the tail of myosin VIIa does not occur through its coiled-coil domain but is mediated by FERM domains [19,23]. This line of evidence indicates that the interaction between SANS CENT and myomegalin also does not occur through coiled-coil domains but is based on the ARM repeat domain of myomegalin which is restricted to the isoform 2 of myomegalin.

In addition to the direct binding of myosin VIIa we have previously shown that the SANS CENT domain mediates SANS homomerization [19]. Our present yeast two-hybrid screen revealed additional 30 potential binding partners of the SANS CENT domain. Myomegalin may compete with these interaction partners in binding to the SANS CENT domain in the cell.

Previous studies have indicated that myomegalin (PDE4DIP) acts as a scaffolding protein found to be associated with centrosomes and the Golgi apparatus [24]. In muscle cells a protein complex containing myomegalin regulates intracellular signaling and trafficking [32]. As known for other proteins interaction of distinct cellular binding partners to the Armadillo repeats may specify the function of myomegalin in various cellular contexts [29]. At the Z-disk of muscle and at the Golgi myomegalin function is closely related to its interplay with PDED4 and the PKA anchoring protein AKAP450 [32–34], which recently has been shown to be required for microtubule nucleation at the Golgi [35]. Interestingly AKAP450 was also identified in our present yeast two-hybrid screen of a retinal library as a putative interacting partner of SANS (Märker et al. unpublished). Thus, SANS may also function in concert with a myomegalin-PDED4-AKAP450 complex in retinal cells.

Previous data demonstrated the association of the USH1G protein SANS with the microtubule cytoskeleton, the centrosome and transport vesicles [13,14,19,21]. Furthermore, there is evidence for a role of SANS in microtubule-based transport of post-Golgi vesicles in

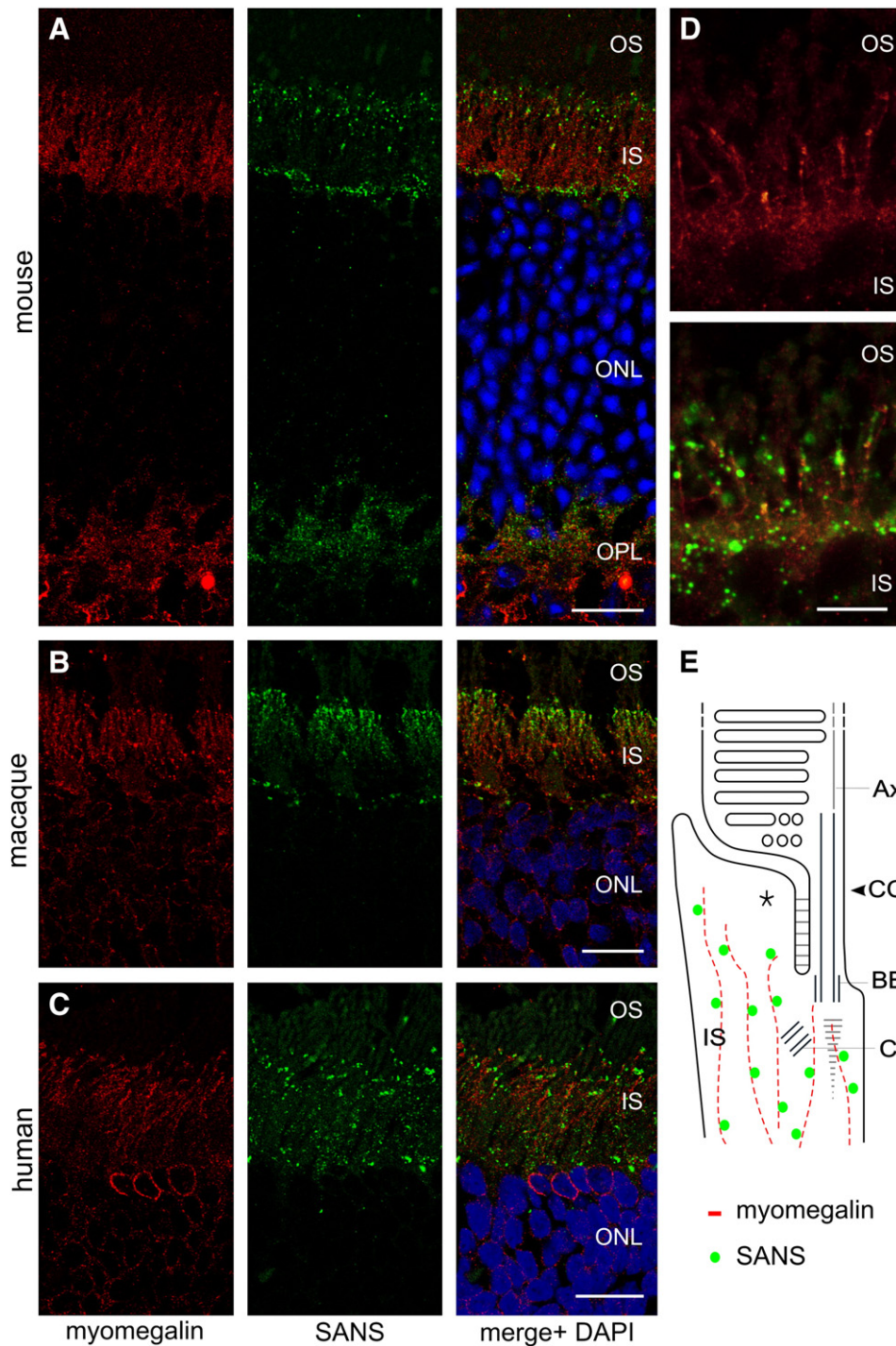


**Fig. 6.** Partial co-localization of myomegalin and SANS in mouse, macaque and human retina. (A–D) Indirect immunofluorescence labeling of myomegalin (red) and SANS (green) in longitudinal cryosections through mouse, macaque and human retina. Nuclear DAPI staining (blue) reveals the different layers of the retina. (A) In mouse retina myomegalin is localized in a fibrous pattern in the inner segment (IS) and detected in the outer plexiform layer (OPL). SANS is localized in the IS and at the OPL. Myomegalin and SANS are partially co-localized in the IS and OPL. (B) In macaque retina myomegalin is localized in a fibrous pattern in the IS, and detected around the nuclei in the outer nuclear layer (ONL). SANS is localized in the IS. Myomegalin and SANS are partially co-localized in the IS and OPL. (C) In human retina myomegalin is localized in a fibrous pattern in the IS, and detected around the nuclei in the outer nuclear layer (ONL). SANS is localized in the IS. Myomegalin and SANS are partially co-localized in the IS. (D) Zoom of the region of IS and outer segment (OS) by STED microscopical analysis shows myomegalin (red) localization as fibrous pattern in the inner segment. Overlay with SANS (green) shows partial co-localization of myomegalin with SANS punctuate localization. (E) Schematic of the ciliary region of a photoreceptor cell. Localization of myomegalin (red) and SANS (green) is indicated. Scale bars: A–C 15  $\mu\text{m}$ , D 5  $\mu\text{m}$ .

retinal photoreceptor cells [13,14,18]. Here, we show by correlative light and electron microscopy the co-localization of the interacting partners SANS and myomegalin at the microtubule tracks across the photoreceptor inner segment. The inner segmental microtubules are

thought to provide the transport routes for the cytoplasmic dynein mediated vesicle transport [36]. Based on these data we propose a cooperation of the binding partners myomegalin and SANS in vesicle transport along microtubule tracks towards the base of the

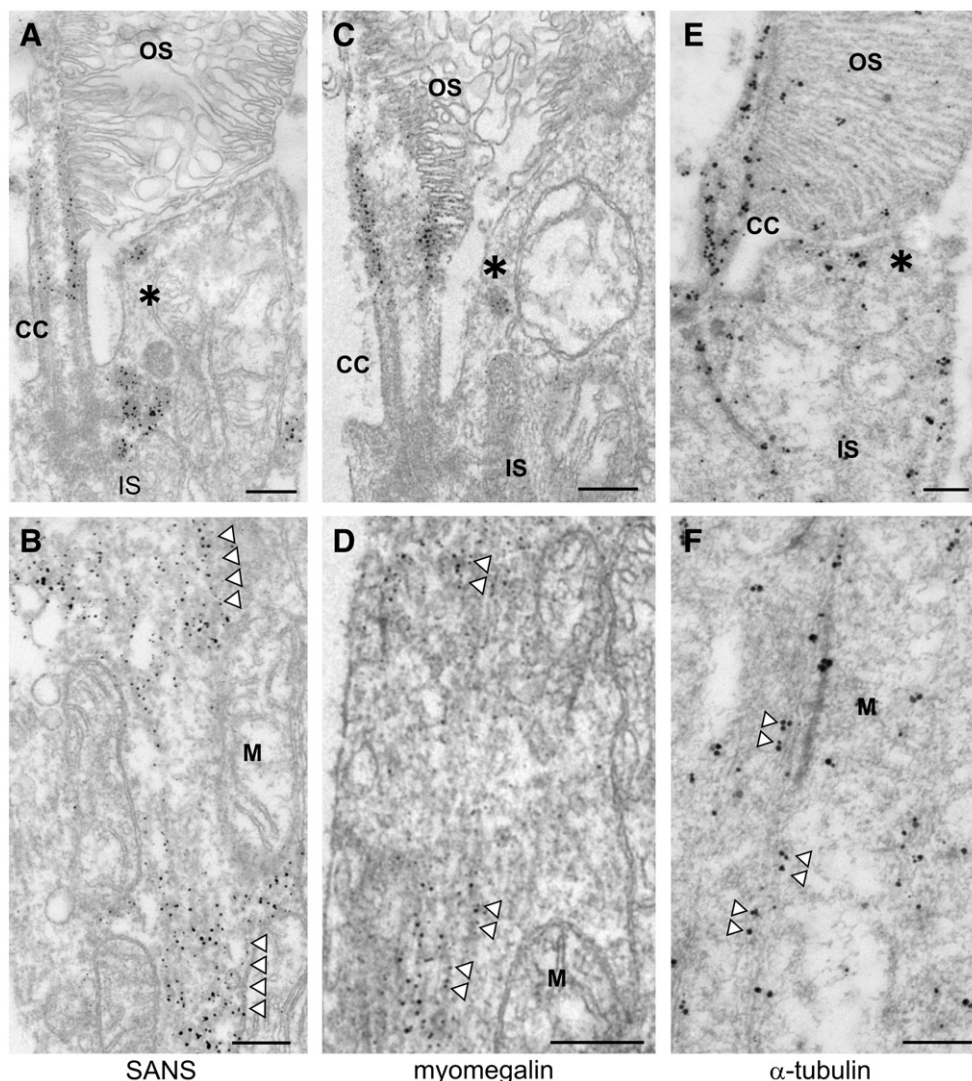


**Fig. 7.** Immunoelectron microscopic localization of SANS, myomegalin and tubulin in human photoreceptor cells. (A, B) Electron micrographs of anti-SANS labeling in longitudinal sections through parts of human photoreceptor cells. SANS localization is found in the apical inner segment extension (asterisk) and at the apical part of the connecting cilium (CC) and at microtubule tracks in the inner segment (IS, arrow heads). (C, D) Electron micrographs of anti-myomegalin labeling in longitudinal sections through parts of human photoreceptor cells. Myomegalin localization is found in the apical inner segment extension (asterisk) and at the apical part of the CC (C) and at microtubule tracks in IS (arrow heads in D). (E–F) Electron micrographs of anti-tubulin labeling in longitudinal sections through parts of human photoreceptor cells. Tubulin localization is found in the apical inner segment (asterisk) and in the CC (E) and along the microtubule tracks in the IS (arrow heads in F). OS; outer segment, M; mitochondrion. Scale bars: 250 nm.

photoreceptor cilium. This target compartment is characterized by the periciliary complex suitable for the cargo transfer between the inner segmental transport and the ciliary delivery to the photoreceptor outer segment [13,37] (Fig. 8). We and others have previously shown that the physical interaction of USH proteins assemble the core complex of this dynamic periciliary protein network [13,16,17]. In this USH protein network we have identified SANS as one of the major scaffolding proteins.

In conclusion, we identified myomegalin as a novel interaction partner of SANS and member of the USH protein interactome [7]. We propose that this interaction may play a role in mediating the microtubule-dependent inner segmental transport of cargo towards the connecting cilium. Here, other members of the USH interactome work together to maintain the efficient cargo transport between the inner segment and outer segment of photoreceptor cells (Fig. 8). Any defect in the interaction of proteins may lead to the disruption of the whole USH network and may result in *retinitis pigmentosa*, the clinical phenotype in the retina of USH1 patients.

#### Disclosure statement

All authors disclose any actual or potential conflict of interest including any financial, personal or other relationships with other people or organizations within three years of beginning the work submitted that could inappropriately influence their work.

#### Role of the funding source

This study was made possible by a scholarship from the 'Stichting Studiefonds UMC St Radboud', which received contributions from the 'Algemene Nederlandse Vereniging ter Voorkoming van Blindheid', the 'Landelijke Stichting voor Blinden en Slechtzienden', MRC Holland, the 'macula Degeneratie Fonds', and the 'Rotterdamse Vereniging Blindenbelangen.' This work was supported by the DFG (to U.W.), Forschung contra Blindheit – Initiative Usher Syndrom (to H.K., T.M. and U.W.), ProRetina Deutschland (to U.W.), the FAUN-Stiftung, Nurnberg (to U.W.), European Community FP7/2009/241955 (SYSCILIA) (to H.K. and U.W.), the LSBS (to

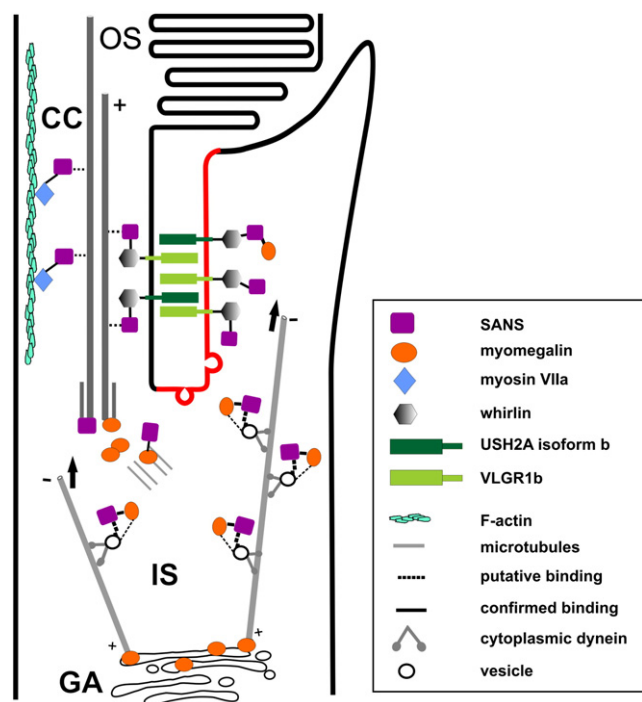


**Fig. 8.** Hypothesis of myomegalin participation in inner segmental transport processes in photoreceptor cells. Due to its direct interaction with SANS myomegalin can be integrated into the USH network. Therefore, putative functions of the myomegalin-SANS partnership in photoreceptor transport processes can be assumed. Vesicles from the Golgi, destined to the outer segment can either be transported by myomegalin and SANS up to the cargo reloading point at the basal body. On the other hand, SANS and myomegalin mediated transport of cargo from the Golgi network can be directed to the periciliary target membrane (red line) where vesicles dock and fuse to the apical inner segment membrane.

H.K.). Funding sources did not participate in study design, in the collection, analysis, and interpretation of data; in the writing of the report; and in the decision to submit the paper for publication.

**Acknowledgements**

Authors thank Dr. Philipp Trojan, Dr. Michiel van Wyk, and Tina Sedmak for critical reading of this manuscript, Tobias Goldmann, Ulrike Maas, Elisabeth Sehn, and Gabi Stern-Schneider for excellent technical assistance.

**References**

[1] J. Reiners, K. Nagel-Wolfrum, K. Jürgens, T. Märker, U. Wolfrum, Molecular basis of human Usher syndrome: deciphering the meshes of the Usher protein network provides insights into the pathomechanisms of the Usher disease, *EXP. EYE RES.* 83 (2006) 97–119.

[2] I. Ebermann, R. Wilke, T. Lauhoff, D. Lubben, E. Zrenner, H.J. Bolz, Two truncating USH3A mutations, including one novel, in a German family with Usher syndrome, *Mol. Vis.* 13 (2007) 1539–1547.

[3] S.L.H. Davenport, G.S. Omenn, The Heterogeneity of Usher Syndrome, 1977.

[4] C. Petit, Usher syndrome: from genetics to pathogenesis, *Annu. Rev. Genomics Hum. Genet.* 2 (2001) 271–297.

[5] Z.M. Ahmed, R.J. Morell, S. Riazuddin, A. Gropman, S. Shaukat, M.M. Ahmad, S.A. Mohiddin, L. Fananapazir, R.C. Caruso, T. Husnain, S.N. Khan, S. Riazuddin, A.J. Griffith, T.B. Friedman, E.R. Wilcox, Mutations of MYO6 are associated with recessive deafness, *DFNB37*, *Am. J. Hum. Genet.* 72 (2003) 1315–1322.

[6] H. Kremer, W.E. van, T. Marker, U. Wolfrum, R. Roepman, Usher syndrome: molecular links of pathogenesis, proteins and pathways, *Hum. Mol. Genet.* 15 (Spec No 2) (2006) R262–R270.

[7] U. Wolfrum, Protein networks related to the Usher syndrome gain insights in the molecular basis of the disease, in: A. Satpal (Ed.), *Usher Syndrome: Pathogenesis, Diagnosis and Therapy*, Nova Science Publishers, 2011, pp. 1–23.

[8] D. Weil, A. El Amraoui, S. Masmoudi, M. Mustapha, Y. Kikkawa, S. Laine, S. Delmaghani, A. Adato, S. Nadifi, Z.B. Zina, C. Hamel, A. Gal, H. Ayadi, H. Yonekawa, C. Petit, Usher syndrome type 1 G (USH1G) is caused by mutations in the gene

encoding SANS, a protein that associates with the USH1C protein, harmonin, *Hum. Mol. Genet.* 12 (2003) 463–471.

[9] A. El Amraoui, C. Petit, Usher I syndrome: unravelling the mechanisms that underlie the cohesion of the growing hair bundle in inner ear sensory cells, *J. Cell Sci.* 118 (2005) 4593–4603.

[10] U. Muller, Cadherins and mechanotransduction by hair cells, *Curr. Opin. Cell Biol.* 20 (2008) 557–566.

[11] N. Grillet, W. Xiong, A. Reynolds, P. Kazmierczak, T. Sato, C. Lillo, R.A. Dumont, E. Hintermann, A. Sczaniecka, M. Schwander, D. Williams, B. Kachar, P.G. Gillespie, U. Muller, Harmonin mutations cause mechanotransduction defects in cochlear hair cells, *Neuron* 62 (2009) 375–387.

[12] M. Schwander, B. Kachar, U. Muller, Review series: the cell biology of hearing, *J. Cell Biol.* 190 (2010) 9–20.

[13] T. Maerker, E. van Wijk, N. Overlack, F.F. Kersten, J. McGee, T. Goldmann, E. Sehn, R. Roepman, E.J. Walsh, H. Kremer, U. Wolfrum, A novel Usher protein network at the periciliary reloading point between molecular transport machineries in vertebrate photoreceptor cells, *Hum. Mol. Genet.* 17 (2008) 71–86.

[14] N. Overlack, T. Maerker, M. Latz, K. Nagel-Wolfrum, U. Wolfrum, SANS (USH1G) expression in developing and mature mammalian retina, *Vision Res.* 48 (2008) 400–412.

[15] E. van Wijk, F.F. Kersten, A. Kartono, D.A. Mans, K. Brandwijk, S.J. Letteboer, T.A. Peters, T. Marker, X. Yan, C.W. Cremers, F.P. Cremers, U. Wolfrum, R. Roepman, H. Kremer, Usher syndrome and Leber congenital amaurosis are molecularly linked via a novel isoform of the centrosomal ninein-like protein, *Hum. Mol. Genet.* 18 (2009) 51–64.

[16] J. Yang, X. Liu, Y. Zhao, M. Adamian, B. Pawlyk, X. Sun, D.R. McMillan, M.C. Liberman, T. Li, Ablation of whirlin long isoform disrupts the USH2 protein complex and causes vision and hearing loss, *PLoS. Genet.* 6 (2010) e1000955.

[17] J. Zou, L. Luo, Z. Shen, V.A. Chiodo, B.K. Ambati, W.W. Hauswirth, J. Yang, Whirlin replacement restores the formation of the USH2 protein complex in whirlin knockout photoreceptors, *Invest Ophthalmol. Vis. Sci.* 52 (2011) 2343–2351.

[18] R. Roepman, U. Wolfrum, Protein networks and complexes in photoreceptor cilia, *Subcell. Biochem.* 43 (2007) 209–235.

[19] A. Adato, G. Lefevre, B. Delprat, V. Michel, N. Michalski, S. Chardenoux, D. Weil, A. El Amraoui, C. Petit, Usherin, the defective protein in Usher syndrome type IIA, is likely to be a component of interstereocilia ankle links in the inner ear sensory cells, *Hum. Mol. Genet.* 14 (2005) 3921–3932.

[20] E. Caberlotto, V. Michel, I. Foucher, A. Bahloul, R.J. Goodyear, E. Pepermans, N. Michalski, I. Perfattini, O. Alegria-Prevot, S. Chardenoux, C.M. Do, J.P. Hardelin, G.P. Richardson, P. Avan, D. Weil, C. Petit, Usher type 1G protein sans is a critical component of the tip-link complex, a structure controlling actin polymerization in stereocilia, *Proc. Natl. Acad. Sci. U. S. A.* 108 (2011) 5825–5830.

[21] M. Zalocchi, J.H. Sisson, D. Cosgrove, Biochemical characterization of native Usher protein complexes from a vesicular subfraction of tracheal epithelial cells, *Biochemistry* 49 (2010) 1236–1247.

[22] J. Yan, L. Pan, X. Chen, L. Wu, M. Zhang, The structure of the harmonin/sans complex reveals an unexpected interaction mode of the two Usher syndrome proteins, *Proc. Natl. Acad. Sci. U. S. A.* 107 (2010) 4040–4045.

[23] L. Wu, L. Pan, Z. Wei, M. Zhang, Structure of MyTH4-FERM domains in myosin VIIa tail bound to cargo, *Science* 331 (2011) 757–760.

[24] I. Verde, G. Pahlke, M. Salanova, G. Zhang, S. Wang, D. Coletti, J. Onuffer, S.L. Jin, M. Conti, Myomegalin is a novel protein of the golgi/centrosome that interacts with a cyclic nucleotide phosphodiesterase, *J. Biol. Chem.* 276 (2001) 11189–11198.

[25] A. Gießl, P. Trojan, A. Pulvermüller, U. Wolfrum, Centrin, potential regulators of transducin translocation in photoreceptor cells, in: D.S. Williams (Ed.), *Cell Biology and Related Disease of the Outer Retina*, World Scientific Publishing Company Pte Ltd, Singapore, 2004, pp. 195–222.

[26] P. Trojan, S. Rausch, A. Giessl, C. Klemm, E. Krause, A. Pulvermuller, U. Wolfrum, Light-dependent CK2-mediated phosphorylation of centrin regulates complex formation with visual G-protein, *Biochim. Biophys. Acta* 1783 (2008) 1248–1260.

[27] U. Wolfrum, Centrin- and  $\alpha$ -actinin-like immunoreactivity in the ciliary rootlets of insect sensilla, *Cell Tissue Res.* 266 (1991) 231–238.

[28] T. Sedmak, E. Sehn, U. Wolfrum, Immunoelectron microscopy of vesicle transport to the primary cilium of photoreceptor cells, *Methods Cell Biol.* 94 (2009) 259–272.

[29] M. Hatzfeld, The armadillo family of structural proteins, *Int. Rev. Cytol.* 186 (1999) 179–224.

[30] P. Burkhard, J. Stetefeld, S.V. Strelkov, Coiled coils: a highly versatile protein folding motif, *Trends Cell Biol.* 11 (2001) 82–88.

[31] J.M. Mason, K.M. Arndt, Coiled coil domains: stability, specificity, and biological implications, *ChemBioChem* 5 (2004) 170–176.

[32] C. Faul, A. Dhume, A.D. Schecter, P. Mundel, Protein kinase A, Ca<sup>2+</sup>/calmodulin-dependent kinase II, and calcineurin regulate the intracellular trafficking of myopodin between the Z-disc and the nucleus of cardiac myocytes, *Mol. Cell Biol.* 27 (2007) 8215–8227.

[33] M. Conti, W. Richter, C. Mehats, G. Livera, J.Y. Park, C. Jin, Cyclic AMP-specific PDE4 phosphodiesterases as critical components of cyclic AMP signaling, *J. Biol. Chem.* 278 (2003) 5493–5496.

[34] K.A. Tasken, P. Collas, W.A. Kimmner, O. Witczak, M. Conti, K. Tasken, Phosphodiesterase 4D and protein kinase a type II constitute a signaling unit in the centrosomal area, *J. Biol. Chem.* 276 (2001) 21999–22002.

[35] S. Rivero, J. Cardenas, M. Bornens, R.M. Rios, Microtubule nucleation at the cis-side of the Golgi apparatus requires AKAP450 and GM130, *EMBO J.* 28 (2009) 1016–1028.

[36] A.W. Tai, J.Z. Chuang, C. Bode, U. Wolfrum, C.H. Sung, Rhodopsin's carboxy-terminal cytoplasmic tail acts as a membrane receptor for cytoplasmic dynein by binding to the dynein light chain Tctex-1, *Cell* 97 (1999) 877–887.

[37] D.S. Papermaster, The birth and death of photoreceptors: the Friedenwald Lecture, *Invest. Ophthalmol. Vis. Sci.* 43 (2002) 1300–1309.